The Astrophysical Journal, 867:34 (10pp), 2018 November 1 https://doi.org/10.3847/1538-4357/aae4e5

NGC 6791: A Probable Bulge Cluster without Multiple Populations*

Sandro Villanova[1], Giovanni Carraro[2], Doug Geisler[1,3,4], Lorenzo Monaco[5], and Paulina Assmann[1]
[1] Departamento de Astronomia, Casilla 160-C, Universidad de Concepcion, Chile; svillanova@astro-udec.cl
[2] Dipartimento di Fisica e Astronomia Galileo Galilei, Universitá di Padova, Vicolo Osservatorio 3, I-35122, Padova, Italy
[3] Instituto de Investigación Multidisciplinario en Ciencia y Tecnología, Universidad de La Serena. Avenida Ral Bitrn S/N, La Serena, Chile
[4] Departamento de Física y Astronomía, Facultad de Ciencias, Universidad de La Serena. Av. Juan Cisternas 1200, La Serena, Chile
[5] Departamento de Ciencias Fisicas, Universidad Andres Bello, Fernandez Concha 700, Las Condes, Santiago, Chile
Received 2018 June 12; revised 2018 September 24; accepted 2018 September 25; published 2018 October 29

Abstract

NGC 6791 is a unique stellar cluster, key to our understanding of both the multiple stellar population phenomenon and the evolution and assembly of the Galaxy. However, despite many investigations, its nature is still very controversial. Geisler et al. found evidence suggesting that it was the first open cluster to possess multiple populations, but several subsequent studies did not corroborate this. It has also been considered a member of the thin or thick disk or even the bulge, and either as an open or globular cluster or even the remnant of a dwarf galaxy. Here we present and discuss detailed abundances derived from high-resolution spectra obtained with UVES at VLT and HIRES at Keck of 17 evolved stars of this cluster. We obtained a mean [Fe/H] $= +0.313 \pm 0.005$, in good agreement with recent estimates, and with no indication of star-to-star metallicity variation, as expected. We also did not find any variation in Na, in spite of having selected the very same stars as in Geisler et al., where an Na variation was claimed. This points to the presence of probable systematics in the lower-resolution spectra of this very high metallicity cluster analyzed in that work. In fact, we find no evidence for an intrinsic spread in any element, corroborating recent independent APOGEE data. The derived abundances indicate that NGC 6791 very likely formed in the Galactic bulge and that the proposed association with the thick disk is unlikely, despite its present Galactic location. We confirm the most recent hypothesis suggesting that the cluster could have formed in the bulge and radially migrated to its current location, which appears to be the best explanation for this intriguing object.

Key words: open clusters and associations: individual (NGC 6791) – stars: abundances

1. Introduction

NGC 6791 is a remarkable, fascinating Milky Way star cluster. From the first detailed studies (Kinman 1965; Spinrad & Taylor 1971), its properties were recognized as being extreme. Its combination of very old age and very high metallicity (~8 Gyr and [Fe/H] $= 0.3-0.4$; Cunha et al. 2015 and references therein) is in fact unique among open clusters in our Galaxy. In addition, in spite of its old age and location at the solar galactocentric distance, this cluster is still one of the most massive ($M \sim 10^4\,M_\odot$) old open clusters known in the Galaxy. Indeed, there is evidence that it has undergone substantial mass loss via tidal interactions (Dalessandro et al. 2015) and was therefore much more massive in the past. Another mystery surrounding its nature is, how did such a high-metallicity object reach its current location 8 kpc from the Galactic center and 1 kpc from the plane? It is an infamous outlier in all age–metallicity relations of Galactic disk objects (e.g., Netopil et al. 2016).

The nature and origin of this cluster are very controversial. An impressive variety of scenarios have been suggested, including the possibility that it is a thick disk cluster (Linden et al. 2017), an extragalactic, strongly mass-depleted dwarf elliptical (Carraro et al. 2006), or a bulge/inner disk star cluster (Jilkova et al. 2012; Martinez-Medina et al. 2018).

Several recent spectroscopic studies have revealed stronger and stronger hints that NGC 6791 was chemically anomalous as well. Hufnagel et al. (1995) found evidence for CN (but not CH) variations in a number of red clump (RC) stars measured using low-resolution spectra, reminiscent of the first signs of multiple populations seen in globular clusters long ago (Hesser et al. 1977). Similar behavior was found for stars covering a range of evolutionary status including the main sequence (MS), red giant branch (RGB), and RC, again from low-resolution spectra from the SEGUE survey (Carrera 2012). The detailed high-resolution study by Geisler et al. (2012) suggested that NGC 6791 actually harbors multiple stellar populations, based on the detection of two groups of evolved stars with significantly different Na abundance. This would make NGC 6791 the first open cluster to possess multiple populations, which until now have been limited to more massive globular clusters (Carretta et al. 2009; Mucciarelli et al. 2016). Together with the suggestion that star formation could have lasted as long as 1 Gyr in the cluster (Twarog et al. 2011), this would make NGC 6791 more similar to Galactic globular or Magellanic Cloud massive clusters, where Na variations or extended star formation histories are routinely found (Baume et al. 2007; Carretta et al. 2010).

However, more recent spectroscopic studies, both high and low resolution (Bragaglia et al. 2014; Boesgaard et al. 2015; Cunha et al. 2015; Boberg et al. 2016; Linden et al. 2017), have not detected any indication of multiple stellar populations. This clearly casts doubt on the reliability of the previous results.

Obviously, our knowledge of the nature, origin, and detailed characteristics of this unique object is sorely lacking. One would like to pin down the origin of such an exotic object and definitively determine to which Galactic component it belongs, whether or not it exhibits multiple populations, and its relationship to the Galactic globular and open cluster population. This is the

* Based on observations carried out at La Silla Paranal Observatory under program 095.D-0294.

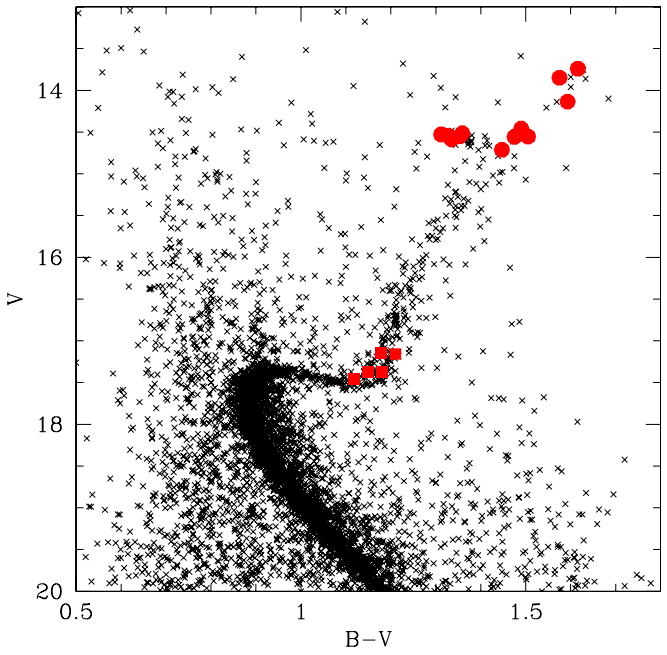

Figure 1. Color–magnitude diagram of NGC 6791. HIRES targets are indicated with red filled squares, UVES targets with red filled circles.

main motivation for the present study. A proper assessment of the cluster chemical characteristics, nature, and origin is still missing, and here we revisit this topic again to try to shed new light on its many mysteries.

To this aim, we collected high-resolution ($R = 47{,}000$) VLT UVES spectra of 14 giants. In order to control uncertainties as much as possible, we selected the very same stars for which previous WIYN Hydra spectra indicated Na abundance variations (Geisler et al. 2012). In addition, we reanalyzed the high-resolution Keck HIRES spectra reported in that paper. Our main goal is to investigate whether our previous results indicating the presence of multiple populations are confirmed or denied. The new abundances also allow us to place the cluster into the larger Galactic context and provide additional information concerning its origin. The paper layout is as follows. In Section 2 we introduce our new observational material and the data reduction, in Section 3 we describe the abundance analysis, in Section 4 we present our results, and in Section 5 we discuss the implications of our results and give our conclusions.

2. Observations and Data Reduction

Our data consist of two sets of high-resolution spectra. The first are the same HIRES spectra collected at the Keck telescope and first analyzed in Geisler et al. (2012). The five stars lie on the reddest extension of the supergiant branch/faintest extension of the RGB (see Figure 1). The second set are data collected at the FLAMES@UVES spectrograph mounted at the VLT-UT2 telescope under the program 095.D-0294(A). In this case, targets are 14 of the upper RGB and RC stars observed previously in Geisler et al. (2012) with the HYDRA instrument on the WIYN telescope. These stars were observed with two fiber configurations. We used the 580 nm setup, which gives a spectral coverage between 4800 and 6800 Å with a resolution of $R = 47{,}000$. This resolution is more than three times higher than the resolution of our previous HYDRA spectra, and the wavelength coverage is many times greater, providing many more lines. The signal-to-noise ratio (S/N) was between 40 and 50 at 6000 Å. Data were reduced using the dedicated pipeline version 5.9.1.[6] Data reduction includes bias subtraction, flat-field correction, wavelength calibration, sky subtraction, and spectral rectification. Radial velocities were measured using the *fxcor* package in IRAF,[7] using a synthetic spectrum as a template. The cluster turns out to have a radial velocity of $-47.0 \pm 0.4\,\mathrm{km\,s^{-1}}$ and a velocity dispersion of $1.5 \pm 0.3\,\mathrm{km\,s^{-1}}$. All stars were confirmed to be cluster members with the exception of T04, for which we measured a radial velocity of $-60.8\,\mathrm{km\,s^{-1}}$. This could indicate a binary nature for this star since in Geisler et al. (2012) it has a radial velocity compatible with the mean value of the cluster. However, we prefer to leave it out of the current analysis. We left out of the analysis also the star T19. Its radial velocity of $-47.41\,\mathrm{km\,s^{-1}}$ is compatible with the cluster mean value, but, because of the low temperature (~3800 K), its spectrum shows strong blending between atomic and molecular lines and a continuum level that is very difficult to determine. Table 1 lists the basic parameters of the 12 remaining stars: ID from Stetson's photometry (Stetson et al. 2003), ID from Geisler et al. (2012), J2000.0 coordinates (R.A. and decl. in degrees), heliocentric radial velocity RV_H ($\mathrm{km\,s^{-1}}$), and *B, I, V, J, H, K_s* magnitudes.

3. Abundance Analysis

The abundance analysis was performed using ATLAS9 atmospheric models (Kurucz 1970) and the local thermodynamic equilibrium (LTE) program MOOG (Sneden 1973). Si I, Ca I, Ti I, Ti II, Cr I, Fe I, Fe II, and Ni I abundances were estimated using the equivalent width (EW) method. EWs were measured manually adjusting a Gaussian to each spectral line. Lines affected by blending or telluric contamination were rejected. The main problem in this case was the continuum determination, due to the very high metallicity. We solved this by comparing our spectra with synthetics calculated using the same atmospheric parameters as the targets and adopting as continuum only those portions of the observed spectra where the corresponding synthetic was $\leqslant 1\%$ below the theoretical continuum. Na I, Mg I, Al I, Y II, La II, and Eu II abundances were obtained using the spectrum synthesis method. For this purpose, five synthetic spectra were generated for each line with 0.25 dex abundance steps in between them and then compared with the observed spectrum. The line list and the methodology we used are the same used in previous papers (e.g., Geisler et al. 2012; Villanova et al. 2013), so we refer to those articles for a detailed discussion of this particular point. Here we emphasize the fact that we took hyperfine splitting into account for Ba as in our previous studies. This is particularly important because Ba lines are very strong and hyperfine splitting helps to remove the line-core saturation, producing a change in the final abundance as estimated by the spectrum synthesis method by up to 0.1 dex. Also Y and Eu are affected by hyperfine splitting, but their lines are much weaker compared to Ba, and the line-core saturation is negligible. On the other hand, Na is an element affected by non-LTE (NLTE) effects. For this reason we checked for NLTE corrections using

[6] See http://www.eso.org/sci/software/pipelines/.

[7] IRAF is distributed by the National Optical Astronomy Observatory, which is operated by the Association of Universities for Research in Astronomy, Inc., under cooperative agreement with the National Science Foundation; see Tody (1993).

Table 1
ID, Coordinates, Radial Velocities, and Magnitudes of the Observed Stars

ID	ID(G12)	R.A.(2000.0) (deg)	Decl.(2000.0) (deg)	V_R (km s^{-1})	B (mag)	V (mag)	I (mag)	J (mag)	H (mag)	K (mag)
12630	T06	290.15787500	37.74702778	−47.89	15.841	14.529	13.168	12.222	11.606	11.435
13579	T14	290.17020833	37.77275000	−48.60	15.904	14.551	13.217	12.108	11.503	11.344
14235	T18	290.17804167	37.85213889	−47.40	15.874	14.515	13.176	12.248	11.648	11.488
14537	T09	290.18154167	37.78391667	−49.57	16.160	14.713	13.230	12.174	11.503	11.325
16927	T03	290.20695833	37.73555556	−48.11	15.923	14.588	13.264	12.273	11.685	11.500
18113	T15	290.21916667	37.74125000	−44.72	15.729	14.136	12.373	11.135	10.417	10.185
18243	T05	290.22037500	37.75927778	−45.21	15.874	14.546	13.235	12.280	11.669	11.513
18444	T07	290.22245833	37.80788889	−47.34	15.357	13.741	11.962	10.732	9.962	9.769
18772	T17	290.22579167	37.77466667	−45.18	16.059	14.554	12.988	11.857	11.170	10.978
19234	T12	290.23045833	37.72100000	−47.16	16.032	14.557	13.027	11.945	11.269	11.088
21447	T11	290.25470833	37.70383333	−46.70	15.949	14.459	12.890	11.821	11.130	10.938
22559	T10	290.26779167	37.78858333	−46.43	15.424	13.849	12.191	11.014	10.310	10.102
08506	T31	290.22495833	37.77830556	−46.30	18.329	17.150	15.954	14.770	14.332	14.335
09609	T32	290.23833333	37.79583333	−38.80	18.368	17.158	15.923	15.128	14.512	14.357
11014	T33	290.25620833	37.74683333	−44.80	18.575	17.457	16.330	15.577	15.210	14.904
11092	T34	290.25733333	37.77563889	−46.30	18.553	17.372	16.164	15.394	14.727	14.623
12383	T35	290.27687500	37.76058333	−48.00	18.520	17.370	16.210	…	…	…

Note. The typical error in radial velocity is 0.5 km s^{-1}. G12 indicates Geisler et al. (2012) identification. See the text for details.

the INSPEC[8] database. The corrections turned out to be very similar for all the stars, in the range of −0.10 to −0.14 dex. We decided to apply a common correction of −0.12 dex to all the targets.

At odds with Geisler et al. (2012), here we could not measure [O/Fe] because the oxygen line at 6300 Å was too badly blended with the oxygen atmospheric emission line that falls exactly at the center of the stellar line given the geocentric radial velocity at the time of our observations.

As initial atmospheric parameters, we used the values reported in Geisler et al. (2012). Here we just want to remember that those parameters are based on multicolor photometry. $T_{\rm eff}$ was derived from $B-V$, $V-I$, $V-J$, $V-H$, $V-K$, $J-H$, and $J-K$ colors adopting a reddening of $E(B-V)=0.13$. Surface gravities (log(g)) were obtained from the canonical equation:

$$\log\left(\frac{g}{g_{\odot}}\right)=\log\left(\frac{M}{M_{\odot}}\right)+4\log\left(\frac{T_{\rm eff}}{T_{\odot}}\right)-\log\left(\frac{L}{L_{\odot}}\right),$$

where the mass M was assumed to be 1.13 and 1.05 $M_{\odot}$ for RGB and RC/AGB stars, respectively. Luminosity $L/L_{\odot}$ was obtained from the absolute magnitude $M_{\rm V}$ assuming an apparent distance modulus of $(m\text{–}M)_{\rm V}=13.44$. Finally, the microturbulent velocity ($v_{\rm t}$) was obtained from the relation of Gratton et al. (1996) that takes both temperature and gravity into account.

Since we used high-quality photometry and seven color combinations for the temperature determination, the random errors are very low. The temperature error was obtained by comparing the individual color-based determinations for each star, while the errors in gravity and microturbulence were obtained by applying error propagation to the previous equations assuming an internal mass uncertainty of 0.05 $M_{\odot}$. We obtained $\sigma_{T_{\rm eff}}=10$ K, $\sigma_{\log(g)}=0.05$ dex, and $\sigma_{v_t}=0.04$ km s^{-1}. With respect to our previous analysis, here we have spectra with much higher resolution and many more Fe lines (65–75 per star), so the error due to the S/N is very low, of the order of $\sigma_{\rm [Fe/H]}0.01$ dex.

Having so many available Fe lines, we also tried to derive the atmospheric parameters spectroscopically, where $T_{\rm eff}$, log(g), and $v_{\rm t}$ were readjusted and new atmospheric models calculated in an interactive way in order to remove trends in excitation potential and reduced EW versus abundance for $T_{\rm eff}$ and $v_{\rm t}$, respectively, and to satisfy the ionization equilibrium between Fe I and Fe II for log(g). In this case the [Fe/H] value of the model was changed at each iteration according to the output of the previous abundance analysis. However, the final result was not as accurate as that based on photometry because errors in temperature and microturbulence were much higher (∼50−60 K and ∼0.10−0.15 km s^{-1}, respectively). That is because in this line-by-line analysis the spread of results from the many Fe lines was relatively large, and so it was very difficult to remove outliers for a proper spectroscopic parameter determination. We conclude that the use of photometric-based parameters was the best way to pursue our analysis in order to have the smallest internal error.

However, photometric-based parameters are affected by systematic errors since we assumed a reddening and a distance modulus that are uncertain. The microturbulence scale we used was also based on an equation that could contain systematics. In order to remove such systematics as much as possible, we used the same spectroscopic analysis described above, but with a variation. First of all, we put all the single Fe I/II and Ti I/II abundances of all the stars together. For this purpose we calculated normalized abundances (Δ[El./H)], where we subtracted the mean abundance of the star from the Fe I/II and Ti I/II abundances obtained from each single line. Then, we applied to the photometric-based $T_{\rm eff}$, log(g), and $v_{\rm t}$ scales three zero-point corrections ($\Delta T_{\rm eff}$, Δlog(g), and Δv_t) in order to remove trends in excitation potential and reduced EW versus abundance (for the temperature and the microturbulence scales, respectively) and to satisfy the ionization equilibrium between Fe I and Fe II and between Ti I and Ti II simultaneously (for the log(g) scale). Since our targets cover different evolutionary

[8] version 1.0 (http://inspect.coolstars19.com)

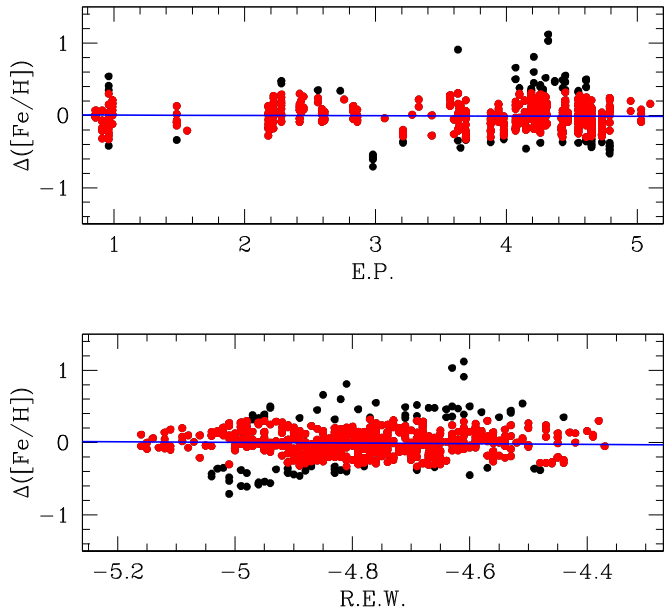

Figure 2. Δ[Fe/H] abundances vs. excitation potential (E.P.; top panel) and vs. reduced EW (R.E.W.; bottom panel) for all RGB and RC stars. Rejected points are indicated by black circles. See the text for more details.

phases, we decided to divide them into three groups: RC stars, upper RGB stars, and lower RGB stars. We applied the procedure described above to the three groups separately. RC and upper RGB stars turned out to require the same zero-point corrections, while for lower RGB stars the zero-point correction for microturbulence is slightly lower. The result is reported in Figure 2 for RC and upper RGB stars together. The zero-point corrections we had to apply are the following: $\Delta T_{\rm eff} = -25$ K and $\Delta\log(g) = -0.30$ dex for all the groups, $\Delta v_t = +0.13$ km s^{-1} for RC and upper RGB stars, and $\Delta v_t = +0.08$ km s^{-1} for lower RGB stars. We also applied a σ-clipping rejection method. Rejected abundances are in black, while good abundances are in red.

A great advantage of this method is that it allows identification of outliers (i.e., those lines that for blending or other reasons give relatively extreme abundances) efficiently, which can then be easily removed. In this way the final abundances are greatly improved. We applied the same outlier removing process also to the other elements measured by EWs. We do not show these plots here, but they are similar to Figure 2. The final abundances of Si, Ca, Ti, Cr, Fe, and Ni were calculated using only the lines with good abundances left after the σ-clipping rejection. For Ti, we give the mean of the Ti I and Ti II abundances. The results of the abundance analysis are reported in Table 2.

As a final comment, we underline the fact that microturbulence is a critical parameter because of the high metallicity and the relatively low temperature of our stars, and final abundances depend strongly on it. This is the first time that this parameter is obtained directly from the spectra of NGC 6791 stars and not assumed from some equation. This makes us confident that the final [Fe/H] values we give are as robust as possible.

Error analysis has been conducted assuming star #18243 as representative of the sample. We varied its $T_{\rm eff}$, $\log(g)$, [Fe/H], and $v_{\rm t}$ according to the internal atmospheric errors reported above and redetermined the abundances. We also performed an error analysis assuming more conservative errors on the parameters, that is, $\sigma_{T_{\rm eff}} = 50$ K, $\sigma_{\log(g)} = 0.20$ dex, $\sigma_{v_t} = 0.10$ km s^{-1}, and $\sigma_{\rm [Fe/H]} = 0.05$ dex. Results are shown in Table 3, including the error due to the noise of the spectra. Errors obtained using the more conservative errors on the parameters are those within parentheses. Error due to the noise was obtained for elements whose abundance was obtained by EWs, as the errors on the mean given by MOOG, and for elements whose abundance was obtained by spectrum synthesis, as the error given by the fitting procedure. $\Delta_{\rm tot}$ is the square root of the sum of the squares of the individual errors. In Table 3 for each element we report the observed spread of the sample ($\rm rms_{obs}$) with its error and in the final column the significance (in units of σ) calculated as the absolute value of the difference between $\rm rms_{obs}$ and $\Delta_{\rm tot}$ divided by the error on $\rm rms_{obs}$. This tells us whether the observed dispersion $\rm rms_{obs}$ is intrinsic or due to observational errors. Values larger than 3σ imply an intrinsic dispersion in the species chemical abundance among the cluster stars. Again, values within parentheses are those calculated using the more conservative errors on the parameters.

We performed a further check on the internal consistency of our results by plotting in the top panel of Figure 3 the [Fe/H] abundances of our stars as a function of temperature. No trend is present. For the other elements a similar plot can be misleading since their abundances are not as accurate as those for iron and can deviate significantly from the mean value of the cluster, creating a false trend. This is because their abundances are based on fewer spectral lines than Fe, implying that some outliers can still be present in spite of the procedure we applied to remove them as much as possible. Because of this, a global plot is more significant. For this purpose, first of all we considered each element separately and subtracted from the abundance of each star the mean value of the cluster, obtaining what we call normalized abundance ratios (Δ[El./Fe]). Then we plot all the normalized abundance ratios together as a function of temperature in the bottom panel of Figure 3. The advantage of this procedure is that we have a much larger sample and abundance ratios that deviate significantly from the mean value of the cluster have a much lower impact on the final trend. Figure 3 reveals that in fact no temperature trend is present for our normalized abundances either.

4. Results

The mean iron content we obtained is

$$[\rm Fe/H] = +0.313 \pm 0.003,$$

with a dispersion of

$$\sigma_{\rm [Fe/H]} = 0.020 \pm 0.003.$$

Reported errors are errors on the mean. This value is lower than our previous measurement of [Fe/H] $= +0.42 \pm 0.01$ (Geisler et al. 2012), but well in line with recent determinations. The difference with respect to Geisler et al. (2012) is mainly due to the different microturbulence scale we adopted here. Bragaglia et al. (2014) find [Fe/H] $= +0.34 \pm 0.02$, Boesgaard et al. (2015) derive $+0.30 \pm 0.02$, Cunha et al. (2015) derive $+0.34 \pm 0.06$, and Linden et al. (2017) derive $+0.31 \pm 0.01$. The latter three studies all use the same APOGEE data set. Our results agree nicely with Boesgaard et al. (2015) and Linden et al. within 1σ, while both Bragaglia et al. (2014) and Cunha et al. (2015) have a slightly higher

Table 2
Parameters and Abundances of the Observed Stars

ID	$T_{\rm eff}$ (K)	log(g)	v_t (km s^{-1})	[Fe/H] (dex)	[Na/Fe] (dex)	[Mg/Fe] (dex)	[Al/Fe] (dex)	[SiFe] (dex)	[Ca/Fe] (dex)	[Ti/Fe] (dex)	[Cr/Fe] (dex)	[Ni/Fe] (dex)	[Y/Fe] (dex)	[Ba/Fe] (dex)	[Eu/Fe] (dex)
12630	4376	1.99	1.31	0.28	−0.05	0.24	0.20	⋯	−0.06	0.09	0.07	0.16	0.22	0.06	0.10
13579	4402	2.02	1.31	0.31	−0.02	0.12	0.17	−0.01	−0.07	0.06	0.11	0.12	0.06	−0.06	0.12
14235	4444	2.03	1.35	0.32	−0.15	0.18	0.21	−0.08	−0.15	0.25	0.12	0.20	0.07	0.08	0.22
14537	4201	1.96	1.13	0.30	−0.08	0.12	0.32	0.00	0.00	0.20	0.15	⋯	0.16	0.06	0.17
16927	4405	2.03	1.30	0.34	−0.06	0.12	0.26	−0.03	−0.04	0.06	0.06	⋯	0.09	0.02	0.20
18113	3918	1.44	1.25	0.31	−0.07	0.14	0.32	⋯	0.04	0.18	⋯	0.19	0.27	0.00	0.27
18243	4441	2.04	1.34	0.31	−0.06	0.13	0.25	0.03	−0.06	0.09	0.07	0.09	0.12	−0.07	0.12
18444	3926	1.27	1.42	0.34	−0.07	0.17	0.15	0.00	⋯	0.16	0.14	⋯	0.03	0.07	0.10
18772	4095	1.80	1.14	0.34	−0.09	0.16	0.22	0.11	−0.07	0.23	0.08	0.13	0.18	0.11	0.15
19234	4160	1.86	1.17	0.34	−0.06	0.17	0.29	−0.08	−0.06	0.09	0.23	0.08	0.07	0.08	0.24
21447	4139	1.80	1.19	0.32	−0.04	0.17	0.27	0.01	−0.01	⋯	⋯	0.20	0.10	0.00	0.15
22559	4009	1.40	1.40	0.29	−0.15	0.14	0.22	0.04	−0.07	0.12	0.12	0.09	−0.05	0.04	0.14
08506	4674	3.26	0.47	0.31	−0.11	0.13	⋯	0.03	⋯	0.15	0.09	0.14	0.16	0.01	⋯
09609	4647	3.25	0.45	0.31	−0.06	0.22	⋯	0.02	−0.13	0.11	0.09	0.24	0.12	−0.07	⋯
11014	4869	3.49	0.50	0.29	−0.05	0.12	⋯	0.01	⋯	0.06	0.09	0.16	0.11	0.07	⋯
11092	4702	3.37	0.41	0.29	−0.07	0.10	⋯	0.03	−0.05	0.10	0.09	⋯	0.11	0.05	⋯
12383	4775	3.40	0.46	0.33	−0.08	0.16	⋯	−0.03	⋯	⋯	0.10	⋯	0.09	0.06	⋯
Mean				0.314	−0.07	0.15	0.24	0.00	−0.06	0.13	0.11	0.15	0.11	0.03	0.17
Error				0.005	0.01	0.01	0.02	0.01	0.01	0.02	0.01	0.01	0.02	0.01	0.02

Note. The last row gives the mean abundances of the cluster and the relative error of the mean.

Table 3
Estimated Errors on Abundances due to Errors on Atmospheric Parameters and to Spectral Noise for Star #18243 (Column 2 to 6)

El.	$\Delta T_{\rm eff} = 10$ (50) K	Δlog $(g) = 0.05$ (0.20)	$\Delta v_{\rm t} = 0.04$ (0.10) km s^{-1}	Δ[Fe/H] = 0.01 (0.05)	S/N	$\Delta_{\rm tot}$	rms$_{\rm obs}$	Sgn.(σ)
Δ([Na/Fe])	0.01(0.05)	0.01(0.03)	0.01(0.03)	0.00(0.01)	0.05	0.05(0.08)	0.04 ± 0.01	1(4)
Δ([Mg/Fe])	0.00(0.03)	0.02(0.07)	0.00(0.00)	0.02(0.06)	0.04	0.05(0.10)	0.04 ± 0.01	1(6)
Δ([Al/Fe])	0.01(0.04)	0.01(0.03)	0.00(0.01)	0.00(0.01)	0.07	0.07(0.09)	0.05 ± 0.01	2(4)
Δ([Si/Fe])	0.01(0.05)	0.01(0.04)	0.01(0.02)	0.00(0.01)	0.05	0.05(0.08)	0.05 ± 0.01	0(3)
Δ([Ca/Fe])	0.01(0.04)	0.01(0.03)	0.00(0.01)	0.00(0.01)	0.04	0.04(0.07)	0.05 ± 0.01	1(2)
Δ([Ti/Fe])	0.01(0.05)	0.02(0.05)	0.01(0.03)	0.00(0.02)	0.05	0.06(0.09)	0.06 ± 0.01	1(3)
Δ([Cr/Fe])	0.01(0.05)	0.01(0.03)	0.00(0.02)	0.00(0.01)	0.05	0.05(0.08)	0.04 ± 0.01	0(4)
Δ([Fe/H])	0.00(0.03)	0.01(0.03)	0.02(0.03)	0.00(0.01)	0.02	0.03(0.06)	0.020 ± 0.003	3(13)
Δ([Ni/Fe])	0.00(0.02)	0.01(0.03)	0.00(0.00)	0.00(0.01)	0.06	0.06(0.07)	0.05 ± 0.01	1(2)
Δ([Y/Fe])	0.00(0.04)	0.02(0.06)	0.03(0.07)	0.00(0.02)	0.06	0.07(0.12)	0.07 ± 0.01	1(5)
Δ([Ba/Fe])	0.00(0.03)	0.02(0.08)	0.04(0.09)	0.01(0.04)	0.05	0.07(0.14)	0.05 ± 0.01	1(9)
Δ([Eu/Fe])	0.00(0.03)	0.02(0.07)	0.01(0.02)	0.00(0.02)	0.08	0.08(0.11)	0.06 ± 0.01	2(5)

Note. Column (7) gives the total error calculated as the square root of the sum of the squares of Columns (2)–(6). This total error must be compared with the total error as obtained from the observed dispersion (rms) of the data with its error (Column (8)). The last column gives the significance of the difference between the total error for star #18243 and the observed dispersion, in units of σ. Values within parentheses are those calculated using the more conservative errors on the parameters (see the text).

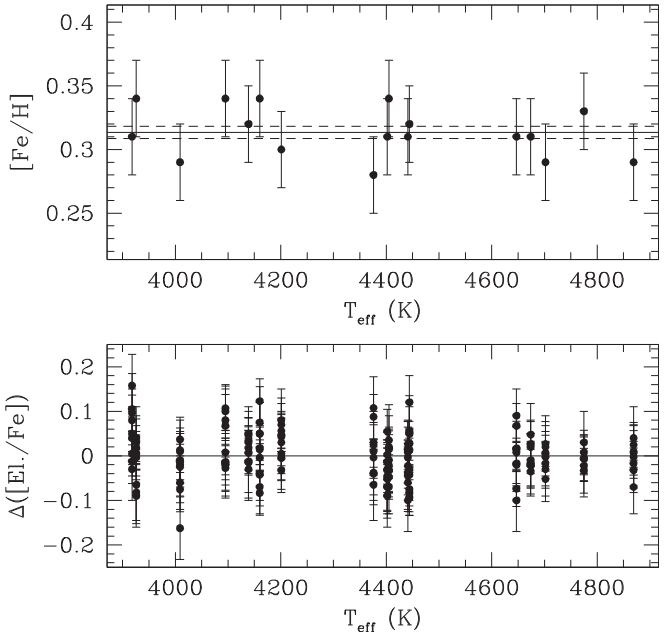

Figure 3. Top panel: [Fe/H] abundances vs. temperature for our sample. The mean value (solid line) and the 1σ error on the mean (dashed lines) are indicated. Bottom panel: normalized Δ[El./Fe] vs. temperature. The zero-slope trend is indicated as a solid line. No trend is visible. See text for more details.

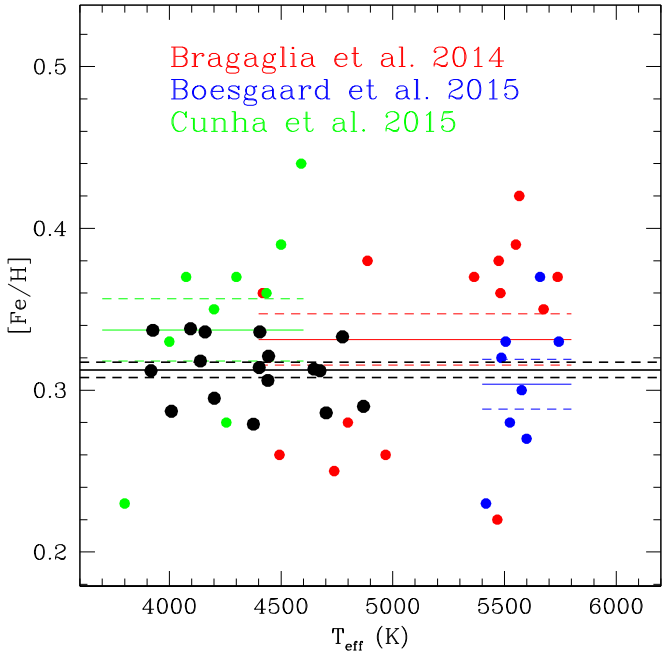

Figure 4. [Fe/H] vs. temperature relation for our data (black points) and three recent spectroscopic studies. Solid lines are the mean values, while dashed lines are the 1σ error on the mean.

metallicity. However, all values are in agreement at the 2σ level. In Figure 4 we report our data (black points) with the results from Bragaglia (2014; red points), Boesgaard et al. (2015; blue points), and Cunha et al. (2015; green points). We notice that both Bragaglia et al. (2014) and Cunha et al. (2015) Fe abundances have a possible trend with temperature.

While our metallicity is not as extreme as some past measurements (most notably the super-metal-rich value of +0.75 reported by Spinrad & Taylor 1971), this metallicity reconfirms NGC 6791 as possibly the most metal-rich open cluster known in the Galaxy, and the only one with such an extreme combination of age and metallicity. The measured iron dispersion in Table 3 agrees well with the expected dispersion due to measurement errors, so we have no evidence for an intrinsic Fe abundance spread, as expected.

Al shows a supersolar value of +0.24 dex, which is larger than any thin- or thick-disk star at the same metallicity. The same behavior is shared by Mg (0.15 dex) and Ti (0.13), although not so extreme. The other two α-elements Si and Ca are on average solar scaled (Si) or slightly subsolar (Ca). The mean α-element content of NGC 6791 based on Mg, Si, Ca, and Ti is solar scaled within the errors:

$$[\alpha/{\rm Fe}] = +0.06 \pm 0.05.$$

As far as iron-peak and heavy elements are concerned, Cr, Ni, Y, and Eu are supersolar, while Ba is solar scaled.

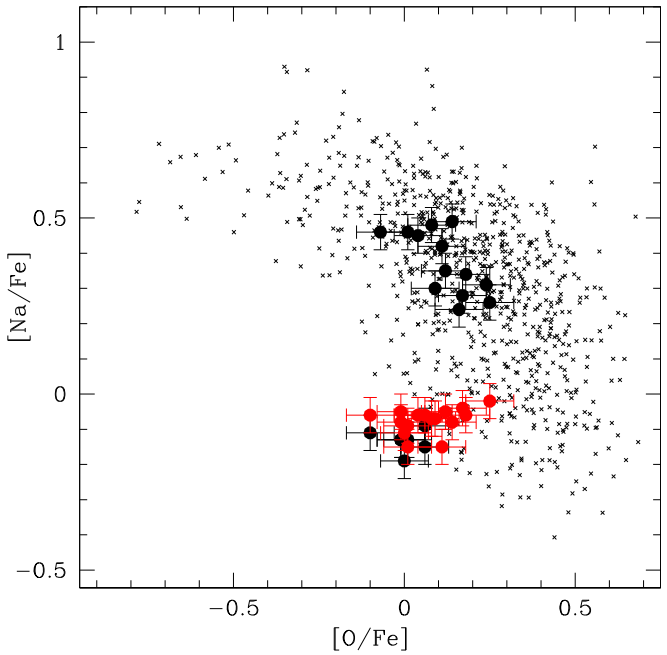

Figure 5. Na–O anticorrelation trend for globular clusters from Carretta et al. (2009; crosses) as a reference. For NGC 6791 we indicate in black the measurements from Geisler et al. (2012) and in red our new determinations.

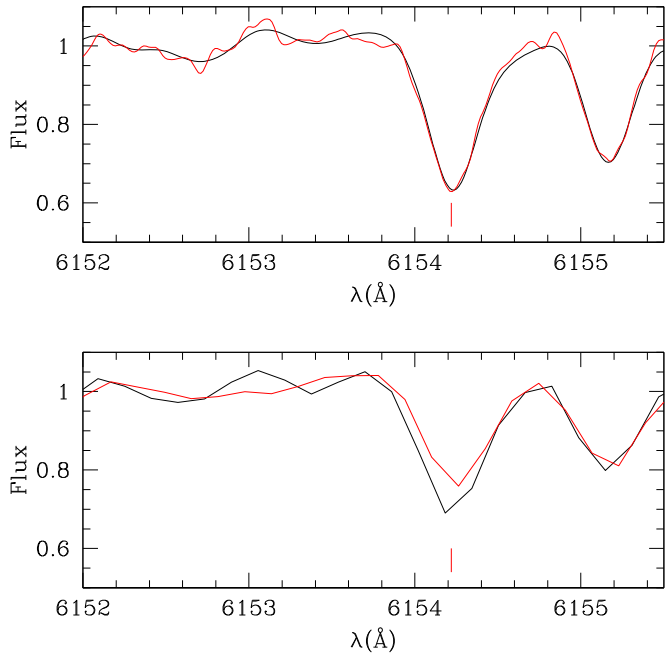

Figure 6. Comparison of UVES spectra (top panel) and Hydra spectra (bottom panel) for the very similar RC stars #T05 (black lines) and #T18 (red lines). The Na line is indicated. In UVES data we find no evidence for any absorption strength variation at odds with what we see in Hydra data. See the text for more details.

4.1. About the Na Spread

One of the chief aims of this paper is to confirm or disprove the very surprising result found in Geisler et al. (2012). On the basis of their Na abundances, they suggested the presence of an intrinsic Na spread and even a slight Na–O anticorrelation, which led to the conclusion that NGC 6791 was the least massive star cluster hosting multiple stellar populations and the first open cluster to display this behavior. In this study, we purposely reobserved the same brightest Geisler et al. (2012) stars, previously observed with Hydra at Kitt Peak, but now using UVES at much higher resolution and much wider wavelength coverage. We compare the present results (red points) with Geisler et al. (2012; black points) in Figure 5. We do not have oxygen here; however, we assume the same Geisler et al. (2012) values since we calculated that the change in the atmospheric parameters affects only marginally (−0.01 to −0.02 dex) the [O/Fe] values we published there. Figure 5 reveals that our current data do not support an Na spread anymore. We investigated possible reasons for this discrepancy and identified the source as most likely due to a reduction problem of the Hydra spectra in Geisler et al. (2012). Figure 6 illustrates this evidence. Red lines are the two spectra of the star #T18, while black lines are the two spectra of the star #T05. These two RC stars have the same atmospheric parameters, so any difference in the strength of a given spectral line directly implies a difference in the abundance of the element that produces the line. The top panel shows the current UVES data, while the bottom panel shows the old Hydra data. The Na line at 6154 Å is indicated. In the Hydra data, the Na lines of the two stars have different strengths, leading to different [Na/Fe] values. On the other hand, UVES data show that the Na lines have the same strength, implying the same Na abundance for the two stars. This means that the Na abundance determinations obtained from the Hydra spectra were likely affected by some kind of instrumental problem, very likely a bad flat-field correction or a bad pixel. We remember here that in Hydra data we had only the Na line at 6140 Å available (the line at 6160 Å was too heavily blended) and that the line sampling was not optimal, making the identification of bad pixels problematic. We conclude that NGC 6791 does not host an Na abundance spread and therefore does not display any evidence for multiple stellar populations. This conclusion is supported also by the other light elements Mg and Al that, according to Table 3, do not show an intrinsic spread. Indeed, there is no evidence for a real spread in any of the 12 elements we measure. This is in accord with the findings of Bragaglia et al. (2014), Boesgaard et al. (2015), and Cunha et al. (2015), but our data have the smallest errors.

Have we thus definitively solved at least one of the mysteries surrounding NGC 6791? But what about the CN spreads seen in previous low-resolution studies by Hufnagel et al. (1995) and Carrera (2012)? Note that Boberg et al. (2016) reanalyzed the SEGUE spectra studied by Carerra and found no strong evidence for any CN (or CH) variations. We cannot derive C, N, or O abundances from our data. But the available APOGEE data and analyses do not show any evidence for intrinsic variation in any of these elements (Cunha et al. 2015). Additional APOGEE data have been obtained to further address this issue, but it appears that NGC 6791, despite our previous claim, does not in fact host multiple populations.

5. Discussion and Conclusions

Recent studies, both observational and theoretical, have addressed once again the issue of the origin of NGC 6791 and its association with the various Galactic components: thin disk, thick disk, or bulge. On the observational side, the comparison of NGC 6791 elemental abundances and abundance ratios with the DR13 release of APOGEE data led Linden et al. (2017) to suggest that NGC 6791 is a member of the Galactic thick disk. Their arguments proceed along three levels. First of all, the

comparison of the metallicity and α ratio seems to suggest a similarity between NGC 6791 and the high-metallicity, high α ratio tail of the Galactic thick disk. Second, the earlier suggestion (Jilkova et al. 2012) that NGC 6791 might have formed close to the bulge is ruled out by the difficulty of displacing such a massive cluster to its actual position. And third, the actual cluster location at 1 kpc above the Galactic plane makes it difficult to envisage a possible connection with the Galactic thin disk. On the theoretical side, Martinez-Medina et al. (2018) provide an independent argument that NGC 6791 might indeed have formed close to the bulge, in the inner 3–5 kpc of the Galaxy, and then suffered radial migration and was displaced to where we observe it today. Based on our new, high-quality data presented in this work, we now reconsider the various arguments in an attempt to provide a more observationally robust scenario for NGC 6791's origin.

First of all, we discuss the possibility that NGC 6791 belongs to the thin disk instead of the thick disk based on its position only. If NGC 6791 was a thick-disk object, it would be the only open cluster associated with this Galactic structure, with the possible addition of *Gaia* 1, which has been recently associated with the thick disk (Koch et al. 2018) on the basis of the very same Linden et al. (2017) argument, namely, that its location is too high to be compatible with the Galactic thin disk. This argument, however, is embarrassingly weak. A wealth of observational data have been accumulated over the past 10 yr that indicate how the Galactic disk, both thin and thick, is not a plain flat structure, but possesses a significant warp and flare in both its gaseous and stellar components and in both its young and old populations. These data are, however, disappointingly neglected. The case of *Gaia* 1 is easy to accommodate (Carraro et al. 2007; Carraro 2018) since it is an outer disk object and the outer thin disk has been repeatedly shown to be significantly warped and to harbor a number of intermediate-age and old open clusters, to which *Gaia* 1 bears much resemblance. There are other open clusters currently located more than 1 kpc above or below the formal Galactic plane ($b = 0°$). However, as in the case of *Gaia* 1, they are all located in the outer part of the Galaxy, and therefore they very likely belong to the warped and flared thin disk (Carraro et al. 2007). The case of NGC 6791 seems more difficult to sort out. In reality, this difficulty is simply apparent because a quick inspection of the warped structure of the disk convincingly shows that at the distance and location of NGC 6791 the disk is actually about 1 kpc off the formal $b = 0^0$ Galactic plane. This is shown in Figure 7, where the Galactic disk as traced by RC stars is shown for scale heights of 0 (solid line), 1, 2, and 3 (dashed lines) in the direction of NGC 6791. From this one can easily infer that NGC 6791 comfortably sits at just over 1 RC scale height from the formal Galactic plane. Since clump stars are genuine Population I objects and trace the Galactic thin disk, the conclusion can be easily drawn that NGC 6791 can also be spatially a member of the Galactic thin disk.

Moving to chemical arguments, we note that the cluster metallicity estimates have been decreasing over the years until recently, and nowadays there is a general consensus that NGC 6791 has [Fe/H] around +0.3 dex. This lower value comes as a consequence of better-quality data and better analysis of the stellar atmospheres in the high-metallicity regime. At [Fe/H] around +0.3, NGC 6791 can be associated either with one of the peaks in the bulge metallicity distribution (Garcia Perez et al. 2018) or with the extreme tails of either the thick or thin

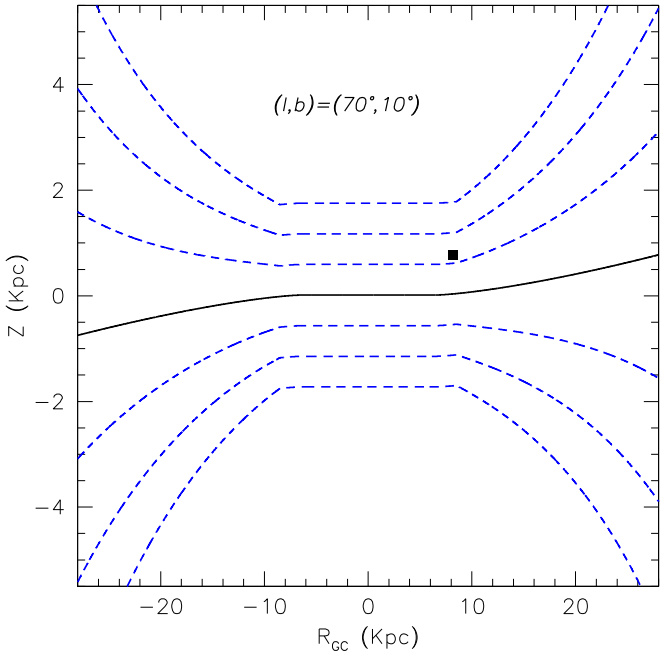

Figure 7. Location in the *X, Z* plane of NGC 6791 with respect to the warped and flared Galactic disk. See text for more details.

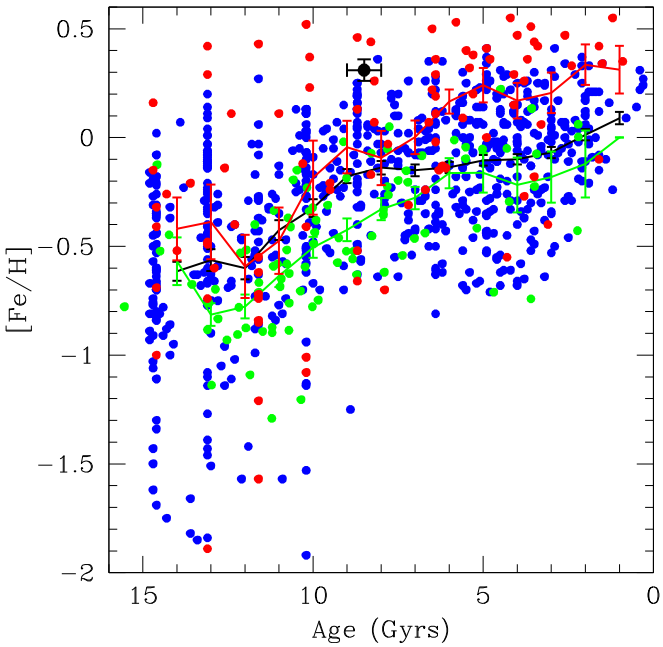

Figure 8. Age–metallicity relations for the thin disk (blue points), thick disk (green points), and bulge (red points). Solid lines with error bars are the respective mean relations. The mean relation for the thin disk is shown in black to be more visible. We assumed an error bar of 0.05 for the NGC 6791 iron content to be conservative (black point).

disks. On purely statistical grounds, it is certainly more likely that it is a typical member of its Galactic component than an extreme one, and therefore a bulge origin is favored. We found [Fe/H] = +0.313 ± 0.005, a value that agrees with the most recent estimates. We can combine this metallicity with the age of the cluster (Buzzoni et al. 2012; 8.5 ± 0.5 Gyr) and compare these data with the age–metallicity relations of the thin and thick disks and the bulge. For this purpose, we used the results of Bensby et al. (2007, 2014, 2017). In Figure 8 blue points

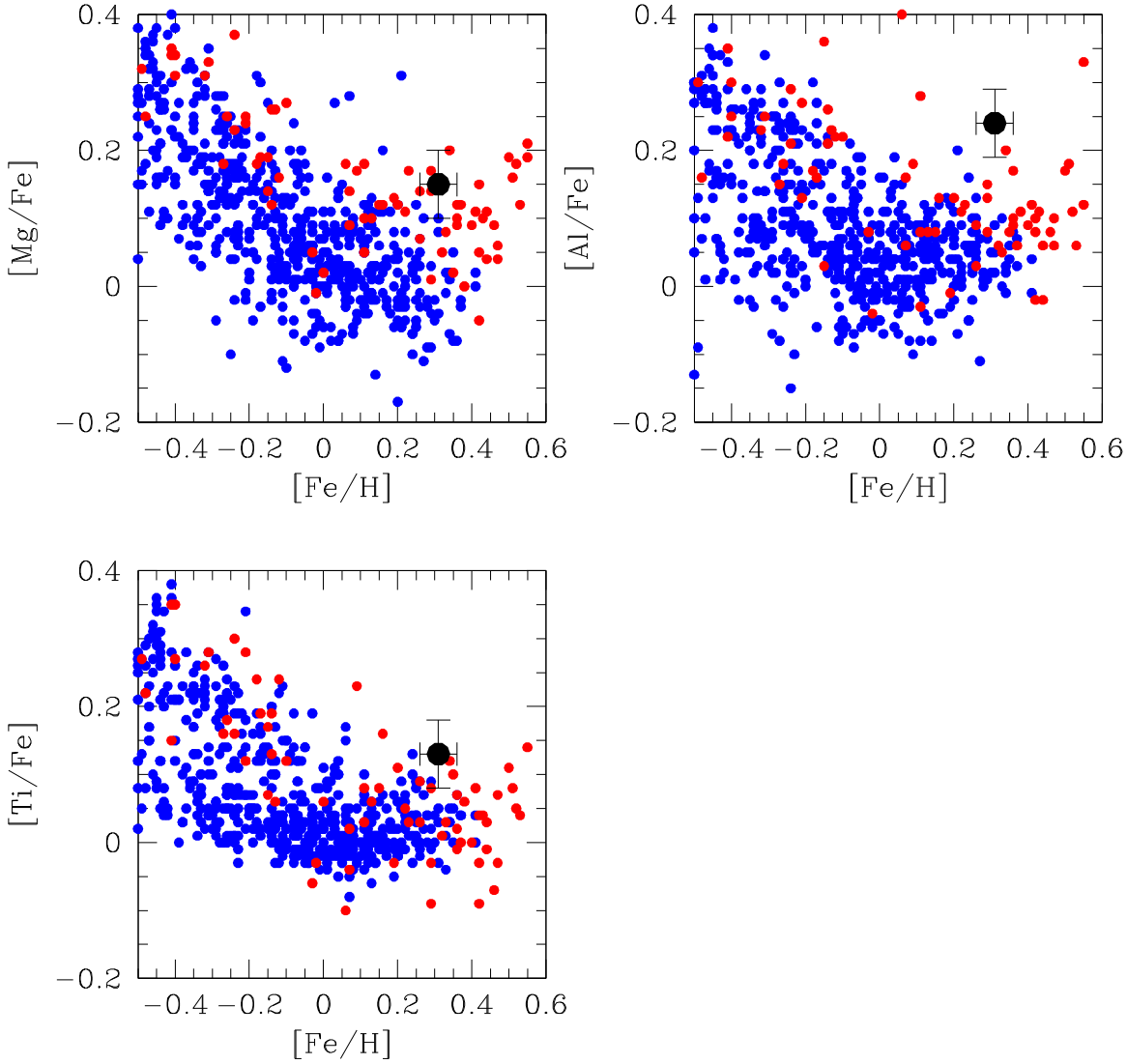

Figure 9. [Mg/Fe], [Al/Fe], and [Ti/Fe] abundances as a function of [Fe/H] for the thin disk (blue points) and the bulge (red points). NGC 6791 is the black circle with error bars. We assumed a conservative error of 0.05 for all elements.

represent the relation for the thin disk, green points the relation for the thick disk, and red points the relation for the bulge. Black, green, and red solid lines with error bars are the mean relations as obtained from the respective data. We used a black line for the thin-disk data (blue points) to make them more visible. NGC 6791 (the black point with error bars) is clearly above all the mean relations. However, note that it lies well above *any* member of the thick disk. This effectively rules it out as a member of this Galactic component. It is also only barely compatible with the thin disk since it lies on the very upper edge of the area covered by thin-disk stars. On the other hand, it lies comfortably within the area covered by bulge stars. Indeed, a few of them are as old or older than NGC 6791 and even more metal-rich. We conclude that, according to this analysis, NGC 6791 most likely belongs to the bulge, although we cannot completely rule out its membership in the thin disk.

Chemistry provides us with further strong evidence for its likely bulge nature. In Figure 9 we plot [Mg/Fe], [Al/Fe], and [Ti/Fe] abundances as a function of [Fe/H] for the thin disk (blue points) and the bulge (red points) from Bensby et al. (2014, 2017). We again see that, as far as Mg and Ti are concerned, NGC 6791 is fully compatible with the bulge, although a possible relation with the thin disk cannot be ruled out, however with a very low probability. In the case of Al, it is very hard to reconcile NGC 6791 with the thin disk, and the association with the bulge is left as the only possible hypothesis. The only weak point of this comparison is that our results are not homogeneous with those from Bensby et al. (2014, 2017). For this reason we look at a totally independent and even larger but still homogeneous data set, that of Schultheis et al. (2017) using 1276 thin-disk stars, 1628 thick-disk stars, and 269 bulge stars from the APOGEE survey. Adding NGC 6791 [Fe/H] and [Mg/Fe] values from APOGEE data ([Fe/H] = +0.34 and [Mg/Fe] = +0.13; see Linden et al. 2017) to their plot of [Mg/Fe] versus [Fe/H], we find that the cluster resides in a region where *only* bulge stars are found. The nearest thin- or thick-disk stars lie many σ away. We report this comparison in Figure 10, where NGC 6791 is represented by the black circle.

This result is further corroborated by yet a second, albeit much smaller, data set—that of Jonsson et al. (2017), where they analyze FLAMES data for a sample of local thick-disk stars versus bulge stars. Our NGC 6791 data place it along the

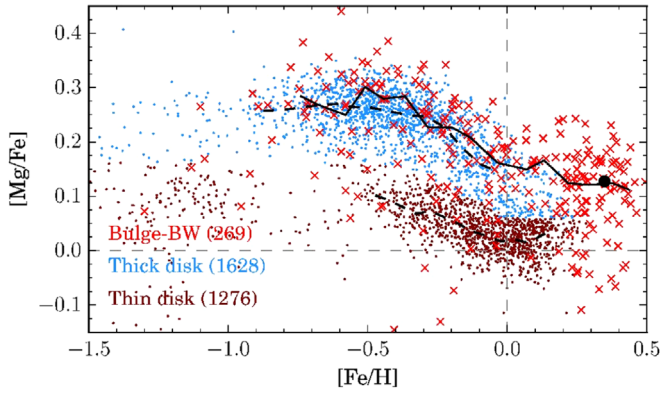

Figure 10. [Mg/Fe] vs. [Fe/H] abundances for thin-disk (blue points), thick-disk (brown points), and bulge (red crosses) stars from Linden et al. (2017). NGC 6791 is represented by the black circle.

trend for bulge stars in the same [Mg/Fe] versus [Fe/H] plane very far away from any thick-disk stars.

The preponderance of the chemical evidence is unequivocal: NGC 6791 is very likely a cluster that was born in the Galactic bulge. The age–metallicity diagram also supports this interpretation. Any possible association with the Galactic thick or thin disks is essentially ruled out. Nevertheless, as we argue below, although probabilities are small, given a large enough sample outliers do occur and NGC 6791, if nothing else, has proven to be an exceptional exception to the rules.

We are left with the conundrum of explaining how an object originating in the bulge has managed to move outward by at least 5 kpc, about a factor of 2 in galactocentric distance, during its lifetime. The problem is exacerbated by the fact that this is not a single star but a massive object, making it less susceptible to effects that would otherwise be quite effective on single stars. Several studies have investigated this scenario dynamically, most recently by Martinez-Medina et al. (2018), who refined and strengthened earlier suggestions by Jilkova et al. (2012) and Dalessandro et al. (2015). They investigated in detail the possibility that NGC 6791 formed in the inner disk or bulge and has radially migrated to its current position. Given its high metallicity and what we know of the thin-disk and bulge metallicity distributions as a function of galactocentric distance (e.g., Garcia Perez et al. 2018), it is likely that it formed at a galactocentric distance of between 3 and 5 kpc and has therefore moved outward by 3–5 kpc over its lifetime. Martinez-Medina et al. (2018) find only a 0.1% probability that this actually happened, given all we know about the cluster and the Galactic potential and dynamics. This is in reasonable agreement with the Jilkova et al. (2012) probability of 0.4%. However, as Martinez-Medina et al. (2018) point out, this means that we only need to have started with a few hundred to a thousand such clusters to find one today that actually achieved this feat. They also find that, in order to survive such radial migration over its lifetime, the original NGC 6791 must have been much more massive, about an order of magnitude. Dalessandro et al. (2015) have indeed uncovered evidence for tidal tails and mass loss from NGC 6791 and estimate that its original mass could have been $\geqslant 10^5\,M_\odot$, more than an order of magnitude larger than its current mass of $5 \times 10^3\,M_\odot$. Martinez-Medina et al. (2018) finally conclude that such a cluster born at a galactocentric distance between 3 and 5 kpc 8 Gyr ago would have a 0.2% probability of being found today where it actually is.

Our observational results combine with these simulations to paint a convincing scenario in which NGC 6791 almost certainly must have formed in the Bulge or inner Disk chemically and has had a slight but non-negligible chance to radially migrate to its current location and orbit dynamically. Thus, this overall scenario of NGC 6791's formation in the inner Galaxy appears very appealing.

S.V. and P.A. gratefully acknowledge the support provided by Fondecyt reg. no. 1170518. D.G. gratefully acknowledges support from the Chilean BASAL Centro de Excelencia en Astrofisica y Tecnologias Afines (CATA) grant PFB-06/2007. D.G. also acknowledges financial support from the Dirección de Investigación y Desarrollo de la Universidad de La Serena through the Programa de Incentivo a la Investigación de Académicos (PIA-DIDULS).

Facility: VLT:FLAMES.

Software: MOOG (Sneden 1973).

ORCID iDs

Sandro Villanova https://orcid.org/0000-0001-6205-1493
Giovanni Carraro https://orcid.org/0000-0002-0155-9434
Doug Geisler https://orcid.org/0000-0002-3900-8208
Lorenzo Monaco https://orcid.org/0000-0002-3148-9836

References

Baume, G., Carraro, G., Costa, E., Mendez, R. A., & Girardi, L. 2007, MNRAS, 375, 1077
Bensby, T., Feltzing, S., Gould, A., et al. 2017, A&A, 605, 89
Bensby, T., Feltzing, S., & Oey, M. S. 2014, A&A, 562, 71
Bensby, T., Zenn, A. R., Oey, M. S., & Feltzing, S. 2007, ApJ, 663, 13
Boberg, O. M., Gerber, J. M., Friel, E. D., et al. 2016, AJ, 151, 127
Boesgaard, A. M., Lum, M. G., & Deliyannis, C. P. 2015, ApJ, 799, 202
Bragaglia, A., Sneden, C., Carretta, E., et al. 2014, ApJ, 796, 68
Buzzoni, A., Bertone, E., Carraro, G., & Buson, L. 2012, ApJ, 749, 35
Carraro, G. 2018, RNAAS, 2, 12
Carraro, G., Geisler, D., Villanova, S., Frinchaboy, P. M., & Majewski, S. R. 2007, A&A, 476, 217
Carraro, G., Villanova, S., Demarque, P., et al. 2006, ApJ, 643, 1151
Carrera, R. 2012, ApJ, 758, 110
Carretta, E., Bragaglia, A., Gratton, R. G., et al. 2009, A&A, 505, 117
Carretta, E., Bragaglia, A., Gratton, R. G., et al. 2010, A&A, 516, 55
Cunha, K., Verne, V. V., Johnson, J. A., et al. 2015, ApJ, 798, 41
Dalessandro, E., Miocchi, P., Carraro, G., Jilkova, L., & Moitinho, A. 2015, MNRAS, 449, 1811
Garcia Perez, A. E., Ness, M., Robin, A. C., et al. 2018, ApJ, 852, 91
Geisler, D., Villanova, S., Carraro, G., et al. 2012, ApJ, 756, 40
Gratton, R. G., Carretta, E., & Castelli, F. 1996, A&A, 314, 191
Hesser, J. E., Hartwick, F. D. A., & McClure, R. D. 1977, ApJS, 33, 471
Hufnagel, B., Smith, G. H., & Janes, K. A. 1995, AJ, 110, 693
Jilkova, L., Carraro, G., Jungwiert, B., & Minchev, I. 2012, A&A, 541, 64
Jonsson, H., Ryde, N., Schultheis, M., & Zoccali, M. 2017, A&A, 598, 101
Kinman, T. D. 1965, ApJ, 142, 655
Koch, A., Hansen, T. T., & Kunder, A. 2018, A&A, 609, 13
Kurucz, R. L. 1970, SAOSR, 309
Linden, S. T., Pryal, M., Hayes, C. R., et al. 2017, ApJ, 842, 49
Martinez-Medina, L. A., Gieles, M., Pichardo, B., & Peimbert, A. 2018, MNRAS, 474, 32
Mucciarelli, A., Dalessandro, E., Massari, D., et al. 2016, ApJ, 824, 73
Netopil, M., Paunzen, E., Heiter, U., & Soubiran, C. 2016, A&A, 585, 150
Schultheis, M., Rojas-Arriagada, A., Garcia Perez, A. E., et al. 2017, A&A, 600, 14
Sneden, C. 1973, ApJ, 184, 839
Spinrad, H., & Taylor, B. J. 1971, ApJ, 163, 303
Stetson, P. B., Bruntt, H., & Grundahl, F. 2003, PASP, 115, 413
Tody, D. 1993, in ASP Conf. Ser. 52, Astronomical Data Analysis Software and Systems II, ed. R. J. Hanisch et al. (San Francicsco, CA: ASP), 173
Twarog, B. A., Carraro, G., & Anthony-Twarog, B. J. 2011, ApJL, 727, L7
Villanova, S., Geisler, D., Carraro, G., Moni Bidin, C., & Muñoz, C. 2013, ApJ, 778, 186